ISSN: 2538-2152; ECOPERSIA 2024;12(3):283-305.

Effect of Geology on the Chemistry of Water in Meymeh River, West of Iran

ARTICLEINFO

Article Type
Original Research

Authors
Ghobad Rostamizad, *Ph.D.*[1]
Zahra Abdollahi, *Ph.D.*[1*]
Haji Karimi, *Ph.D.*[2]
Ahmad Reza Karimi, *Ph.D.*[3]

How to cite this article
Rostamizad R., Abdollahi Z., Karimi H., Karimi AR. Effect of Geology on the Chemistry of Water in Meymeh River, West of Iran. ECOPERSIA 2024;12(3): 283-305.

DOI:
10.22034/ECOPERSIA.12.3.283

[1] Soil Conservation and Watershed Management Research Department, Zanjan Agricultural and Natural Resources Research and Education Center, AREEO, Zanjan, Iran
[2] Watershed and Range Management Department, Agriculture Faculty, Ilam University, Ilam, Iran
[3] Kharazmi University, Tehran, Iran

** Correspondence*
Address: Watershed and Range Management Department, Agriculture Faculty, Ilam University, Ilam, Iran
Tel: 09124420240
Email: Abdollahi.zhr.65@gmail.com

Article History
Received: June 15, 2024
Accepted:August 28, 2024
Published: September 14, 2024

ABSTRACT

Aims: The Meymeh River is fed by several tributaries, which gradually decrease its quality. Considering the construction of the Meymeh reservoir for agricultural use, it is necessary to monitor the spatial and temporal changes in water quality and identify areas where river quality changes.

Material & Methods: Our method was based on analyzing 420 samples over 12 months (2016-2017) in three seasons (low, moderate, and high flow periods) from 35 measuring stations using Spearman's correlation, multivariate statistical analysis, agglomerative hierarchical clustering, and GIS.

Findings: The results showed that crossing the saline evaporite layers (especially the Gachsaran Formation) causes a gradual decrease in water quality from upstream to downstream. So, EC reaches from 400 to more than 3500 µm.cm^{-1} at the confluence of Varazan and Kharvazan tributaries. Besides, the sulfur spring has a mean EC of 21590 µm.cm^{-1} increases EC 3.5 times. Siyoul tributary penetrates under the ground after passing through two saline zones and reappears at a distance of 150 to 200 m with an EC of 187800 µm.cm^{-1}. It was also found that about 50% of the salinity of the Meymeh River is caused by the influence of the Ghadah Sulfur Spring and the Siyoul tributary.

Conclusion: This study has highlighted some options for managing the dam's salinity level. In most cases, one option alone may not have the desired effect, and combining techniques will likely yield the best results.

Keywords: Gachsaran Formation; Geological Effects; Meymeh River; Principal Component Analysis; Water Quality.

CITATION LINKS

[1] Abdollahi Z., Kavian A., ... [2] Faye C. Water Resources and... [3] Mainali J., Chang H. Landscape and anthropo... [4] Wijesiri B., Deilami K., ... [5] Leonardo Mena-Rivera... [6] Sahraei Parizi H., Samani N. Geochemical ev... [7] Barzegar R., Asghari Moghaddam A., Soltani ... [8] Varol M., Gökot B., Bekleyen A., Şen B. Spa... [9] Baba A., Gündüz O. Effect of geogenic facto... [10] Kavian A., Dodangeh S., Abdollahi Z. Annual... [11] Nouri J., Mahvi A., Jahed G., Babaei AJEG R... [12] Khadivi S. Tectonic evolution and growth of... [13] Rezaee P., Salari S. Petrography and minera... [14] Klimchouk A. The dissolution and conversion... [15] Reiss A.G., Gavrieli I., Rosenberg Y.O., Re... [16] Ghadiri A., Hashemi ... [17] Shafiee M., Azizipour M.,... [18] López-López J.A., Mendiguchía C., García-Va... [19] Ma X., Wang L., Yang H., Li N., Gong C. Spa... [20] Melland A.R., Fenton ... [21] Mostafaei A. Application... [22] Qian Y., Migliaccio K.... [23] Barakat A., El Baghdadi... [24] Khan M.Y.A., Gani K.M., Chakrapani G.J. Ass... [25] Grzywna A., Bronowicka... [26] Tokatli C. Water... [27] Custodio M., Peñaloza... [28] Walls S., Binns A.D., Levison J., MacRitchi... [29] Ahmed N., Howlader N., ... [30] Mahdavi M. Applied Hydrology. Tehran Univer... [31] Apha A. WEF (2005) Standard Methods for the... [32] Feizizadeh B., ... [33] Varol MJEP Spatio-temporal changes in surfa... [34] Wang X., Li J., Chen J., ... [35] Liu M., Wang H.-J., Wang H.-Z., Ma S.-N., Y... [36] Kim M., Jang G.-J., Kim J.-H., Lee M. Speak... [37] Bhat S.A., Meraj G., Yaseen S., Pandit A.K.... [38] Yang K., Yu Z., Luo Y., Yang Y., Zhao L., Z... [39] Patil V.B.B., Pinto S.M., Govindaraju T., H... [40] Bean T.A., Sumner P.D., Boojhawon R., Tatay... [41] Zeinalzadeh K., Rezaei E. Determining spati... [42] Simeonov V., Stratis J., Samara C., Zachari... [43] Zheng L.-y., Yu H.-b., Wang Q.-s. Assessmen... [44] Mukherjee I., Singh ... [45] Zhang Q., Li L., Sun R., Zhu D., Zhang C., ... [46] Kurunc A., YÜREKLİ K., ... [47] Ejaz N. Investigation of the Soan River Wat... [48] Ouyang Y., Nkedi-Kizza.... [49] Olsen R.L., Chappell R.W., Loftis J.C. Wate... [50] Piper A.M. A graphic... [51] Clow D.W., Striegl R.G., Dornblaser M. Spat... [52] Razi M.H., Wilopo W., Putra DPE Hydrogeoche... [53] Boulom J., Putra D.P.E., Wilopo W. Chemical... [54] Cloutier V., Lefebvre... [55] Rezaei Moghaddam M.H., Nikjoo M.R., Hejazi ... [56] Kardan Moghaddam H., ... [57] Heshmati M., Gheitury... [58] Kaveh A.R., Habibnejad Roshan M., Shahedi K... [59] Davoudi Moghaddam D., Haghizadeh A., Tahmas...

[DOI: 10.22034/ECOPERSIA.12.3.283]

Introduction

Among the most significant water resources are rivers, vital for providing the water required for various purposes, including drinking, manufacturing, agriculture, and electricity production. Knowledge of the quality of water resources is one of the essential prerequisites for planning and developing water management since the preservation and efficient use of water resources is one of the tenets of any nation's sustainable development. [1].

Appropriate planning and management of water resources are unavoidably required due to the finite water supply, the unequal temporal and spatial distribution of rainfall, global warming, and the rising water demand directly linked to population increases. One of the most important first steps in establishing sensible management of water resources is evaluating the availability and quality of water [2]. As rivers are one of the most valuable surface water sources, monitoring their quality is essential. To assess the health of a watershed and to help with the decision-making process for effective management of present and future pollution, it is crucial to assess the temporal and spatial fluctuations in the quality of surface water [3, 4]. Complex anthropogenic and natural factors influence surface water quality. Natural factors include geological construction, topography, rainfall changes, land cover (vegetation), and seasonal temperature. Although uncontrolled anthropogenic interventions largely contribute to the declining water quality of fresh wafers [5, 6], many researchers have remarked on the importance of natural processes in the degradation of surface water quality [7, 8].

The geology of an area is a critical factor in the overall quality of its water resources [9, 10]. The water-rock interactions and dissolution of many minerals from geological formations result in spatial and temporal variations in river water quality. So, the dominant geological formations are primarily responsible for the overall physicochemical characteristics of local surface and subsurface waters [11]. The Zagros mountains are characterized by a 7–14 km-thick succession of sediments deposited over the northeast edge of the Arabian plate [12]. The Gachsaran Formation, deposited along the axis of the Zagros foreland basin, is one of the important cap rocks of the hydrocarbon reservoir in Iran, which comprises alternations of calcium sulfates, marls, and carbonates. According to field observation and laboratory studies, gypsum/anhydrite, limestone, and marl facies, which are identified as soluble rocks, were identified in the Gachsaran formation [13]. Depending on the rock type, the dissolution process and rock-water interaction process are functions of some properties such as temperature and pressure conditions, texture and structure of the rock, and chemical composition of the water. The solubility of gypsum in pure water, by a simple reversibly two-phase dissociation ($CaSO_4 \cdot 2H_2O \leftrightarrow Ca^{2+} + SO_4^{2-} + 2H_2O$), at 20 °C was reported about 2.531 g. L^{-1} [14]. The more the temperature increases, the more gypsum dissolves in water. Besides, the solubility of gypsum increases with increasing concentrations of some dissolved salts in water, such as sodium chloride [15, 16]. However, the solubility of limestone is impacted by the presence of CO_2 ($CaCO_3 + CO_2 + H_2O \leftrightarrow Ca^{2+} + 2HCO_3^-$), which makes it sensitive to pressure conditions [14, 17].

Despite the wide range of studies conducted on local geological characteristics, a study still needs to be done on the hydrogeological setting of the Gachsaran formation and its environs. Paying more attention to the quality of water environments and different water quality assessment techniques have increasingly developed. Among them,

[DOI: 10.22034/ECOPERSIA.12.3.283]

principal component analysis (PCA) and cluster analysis (CA) are widely considered by researchers in various environmental problems, including assessment of spatial and temporal changes in surface water quality to discover the relationship between the original indicator variables and transform them into independent principal components [3, 14,18].

Barakat et al. [19] used Pearson's correlation, PCA, and CA to assess the spatial and temporal water quality variation and to determine the primary contamination sources in the Oum Er Rbia River and its main tributary. Khan et al. [20] applied CA to assess spatial variability in the water quality of the Ramganga River and its tributaries (Ganga Basin, India). Grzywna and Bronowicka-Mielniczuk [21] Used PCA/FA, HCA, and DA to analyze the spatial and temporal variability of water quality in the Bystrzyca River Basin, Poland. Ma et al. [15] used PCA to assess the spatiotemporal water quality analysis for the Qinhuai River Basin in East China. Tokatli [22] used FA and CA to determine the water quality of the Ergene River Basin and to present the pressure of the Ergene River on the Meriç River. Custodio and Peñaloza [23] used multivariate statistics to analyze data on the spatial and temporal variability of physicochemical indicators of water quality in the Cunas River. These studies showed that the multivariate statistical methods are practical tools to assess underlying relations between the water quality parameters, identify pollution sources, and group similar monitoring stations into clusters with analogous characteristics.

The Meymeh River is in Dehlran City and is south of Ilam Province. Upstream of the river, EC is about 400 μm.cm^{-1}, while it reaches 7000 μm.cm^{-1} in the downstream part. Considering the construction of a dam on the Meymeh River for agricultural use, it is necessary to conduct a comprehensive study of the dam catchment. Therefore, the aims of this study are (1) to monitor the spatial and temporal changes in water quality of the Meymeh River from upstream to downstream, (2) to detect areas where water quality significantly changes, (3) to detect the key factors causing excessive concentrations of contaminants affecting the water quality and (4) to identify opportunities for salinity control and likely impact.

Material & Methods

Study Area

The Meymeh River is one of Iran's most crucial border rivers (Ilam Province), and it eventually entered Iraq. The Meymeh River is in a semi-arid region, with a mean annual temperature above 16 °C and annual rainfall of 450 mm. It emanates from the Kabirkooh mountain, with an area of 1674.40 km^2 (located at 53° 48′ 46″ - 7° 18′ 47″ E, and 6° 42′ 32″ - 10° 19′ 33″ N). The maximum and minimum elevation of the watershed is 2489 m in the Kabirkooh mountain and 174 m in the outlet, respectively (Figure. 1). The climate of the study area is categorized into the semi-arid class based on the Dumarten's aridity factor. Some characteristics,

Table 1) physiographic characteristics including area, watershed length, perimeter, form factor (FF), concentration-time [1], drainage density (Dd), annual precipitation ($\bar{P}$), annual temperature ($\bar{T}$), and mean altitude ($\bar{H}$) of the study area.

Area (km^2)	watershed length (km)	Perimeter (km)	Form factor (FF)	D_d (km.km^{-2})	T_c (h)	$\bar{H}$	$\bar{P}$	$\bar{T}$
1764.40	71.75	325.00	0.34	0.8	9.38	1038.01	518.44	16.88

[DOI: 10.22034/ECOPERSIA.12.3.283]

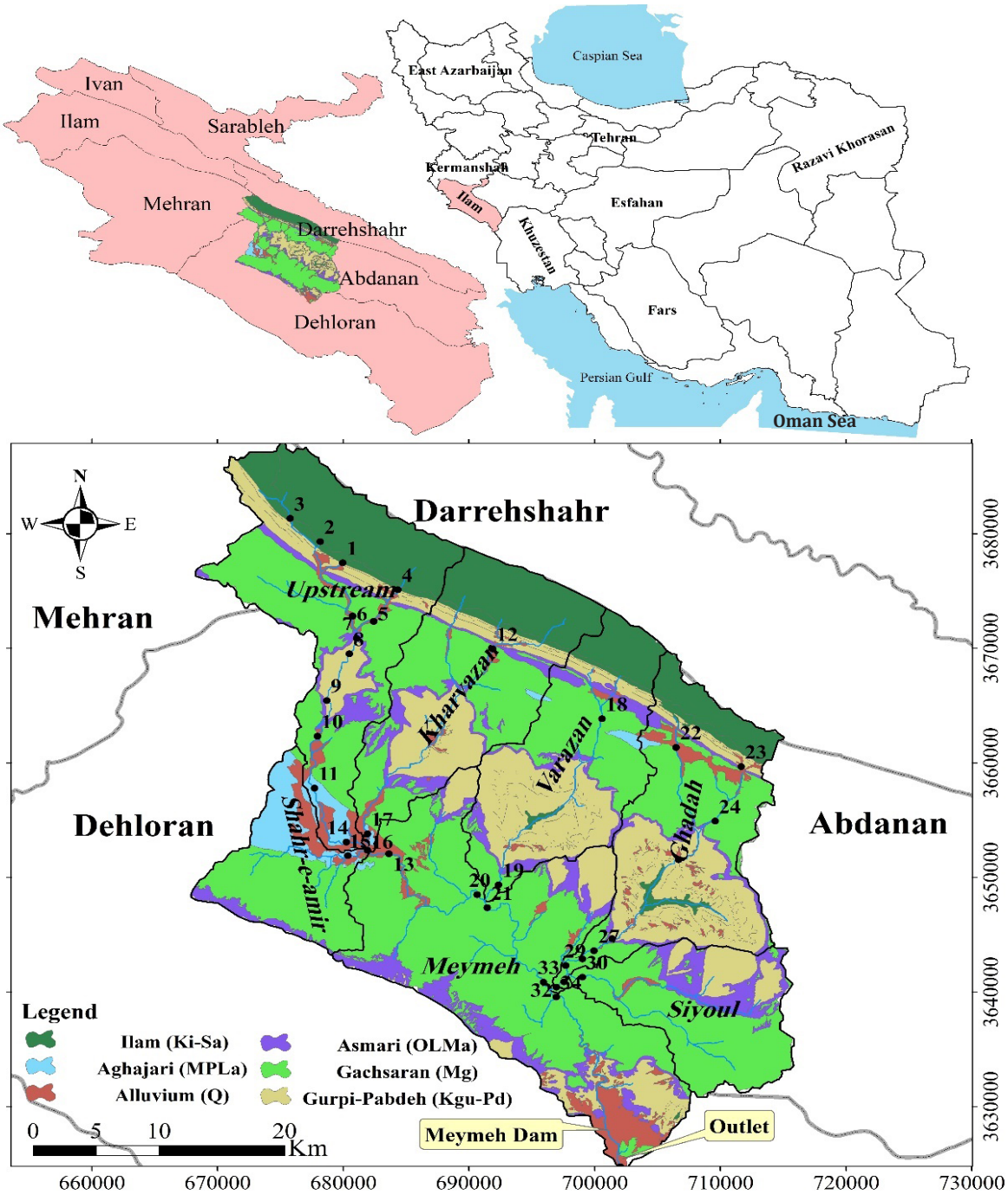

Figure 1) A scheme of the geology and 35 sampling stations along the main river, its tributaries, and at the confluence of each branch in the Meymeh Watershed, Iran.

including area, perimeter, watershed length, form factor (F. F), concentration-time [1], drainage density (Dd), annual precipitation ($\bar{P}$), annual temperature ($\bar{T}$), and mean altitude ($\bar{H}$), are summarized in Table (1). We classified the study area, in terms of land uses, into eight classes, including low-density forest, semi-dense forest, rock, dry land and irrigated farming, semi-dense rangeland, low-density rangeland, and garden (Figure. 2). Semi-dense forests and rangelands cover 56.8 and 27.35 (%) of the region, respectively. They cover 84.15 (%) of the region (Table 2).

[DOI: 10.22034/ECOPERSIA.12.3.283]

Table 2) Area of each land use in the sub-watersheds of the study area (%).

Landuse Unit	Shahr-E-Amir	Kharvazan	Varazan	Siyoul	Ghadah	Upstream	Meymeh	Entire watershed
L-D Forest	0	0	0	0	6.82	0	3.92	1.94
S-D forest	59.64	77.15	70.92	33.61	59.17	75.02	29.27	56.80
Rock	0.0	1.19	11.87	0	12.96	1.27	0.97	4.08
D. Farming	0.0	2.03	10.96	0	15.01	5.57	0.72	5.10
S-DRangeland	22.81	18.30	6.24	66.39	6.05	13.50	54.63	27.35
I. Farming	17.55	1.33	0	0	0	4.27	0.60	2.30
Garden	0.0	0	0	0	0	0.37	0	0.07
L-DRangeland	0.0	0	0	0	0	0	9.90	2.37

Geology

The Meymeh Watershed is part of the 1: 250,000 sheets of Dehloran and Koohdasht in the geological division of Iran. Also, this watershed corresponds to 8 geological sheets of Iran Oil Company with a scale of 1: 50,000, including Kolm (I-5356), Meymeh (II-5356), Bishedaraz (I-5355), Zarangoosh (I-5456), Abdanan (I-5455), Darrehshahr (II-5456), Sarsefidkooh (IV- 5455), Tamtamoo (3-5455). The main structures of the Meymeh Watershed are Kabirkooh, Samand, Anaran, and Siyahkooh anticlines, which developed from north to south with a general northwest-southeast trend, respectively. We presented the coverage area of each formation in the sub-watersheds in Table (3). Accordingly, 44.09 (%) of the watershed is covered by the Gachsaran Formation. The lithology of the Gachsaran Formation comprises evaporate sediments, including gypsum, anhydrite, salt, lime, and bituminous shales with a percentage of green and sometimes red marl [13], which covers a large part of the study watershed. Also, tectonic activities in the Gachsaran Formation cause gypsum and salt layers to move into the cracks and create salt and gypsum accumulations near-fault planes [13]. Dissolution of gypsum and salt layers on or near the surface has reduced river water quality. In addition, fault and tectonics facilitate water access to the deeper parts of the formation or raise salts. Therefore, surface waters are strongly affected by the Gachsaran Formation in the Meymeh Watershed, as a large percentage of the watershed is covered by this formation.

Data Collection

To identify the location and determine geological formations, we used topographic maps with a scale of 1/25000 and geological maps with a scale of 1/100000 as basic maps. The Global Positioning System (GPS) was also used to determine the location of the sampling stations and transfer points to the Geographic Information System (GIS) and Google Earth. We used GIS and ARC HYDRO software to create new maps, extract the watershed's physical characteristics, and perform quantitative analysis.

In this study, water samples were taken monthly from 35 different sampling stations along the main river and its tributaries (Figure. 1) from September 2016 (autumn) to August 2017 (summer).

Thirty-five sampling stations were selected at the confluence of each branch. The characteristics of each station are given in Table (4).

[DOI: 10.22034/ECOPERSIA.12.3.283]

Table 3) Area of each geological formation in the sub-watersheds of the study area (%) extracted from 8 geological sheets with a scale of 1: 50000.

Sub-Watershed	Gachsaran (Mg)	Aghajari (MPLa)	Asmari (OLMa)	ILAM (Ki_Sa)	Gurpi_Pabdeh (KGu_Pd)	Alluvium (Q)
Shahr-e-Amir	60.56	23.47	6.30	0.00	0.00	9.68
Kharvazan	37.96	0.58	8.69	26.35	23.03	3.39
Varazan	33.63	1.04	9.63	13.78	40.81	1.11
Siyoul	65.36	0.00	17.46	0.00	15.98	1.20
Ghadah	32.15	0.42	5.83	15.87	40.04	5.69
Upstream	38.92	3.11	6.27	32.68	13.43	5.60
Meymeh	66.33	0.15	11.76	0.04	13.18	8.55

Table 4) Specifications of 35 sampling stations along the main river, its tributaries, and at the confluence of each branch selected for monthly sampling from September 2016 (autumn) to August 2017 (summer).

Code	Station	X	Y	Code	Station	X	Y
1	Eastern spring	679172	3678669	19	Varazan River	692252	3649372
2	Western Spring	678245	3679501	20	Before Varazan	691231	3648078
3	Seasonal spring	677104	3679599	21	After Varazan	691243	3647811
4	Source of Gourab	684358	3675118	22	Chamasiyab	706486	3661352
5	Gourab River	681254	3671787	23	Gandab	711664	3659673
6	After Gourab	680978	3671474	24	After of Bridge	709595	3654919
7	Before Gourab	680886	3671796	25	Old Bridge	708125	3652628
8	Haftkadeh Hydrometer	681035	3670336	26	Before sulfur Spring	700058	3643601
9	Imamzadeh Fakhreddin	679045	3664923	28	After Sulfur Spring	699821	3643683
10	Gypsum spring on the roadside	678829	3663823	29	Before Sioul	697845	3641626
11	Haftkadeh village	677687	3660154	29	Sulfur Spring	699959	3643601
12	Takhtan	691886	3669952	30	Sioul River	697942	3641447
13	After Kharvazan	682465	3651879	31	After Sioul	697693	3641467
14	Before Shar-e-Amir	681564	3652782	32	Before Meymeh	696590	3640207
15	Shar-e-Amir	681601	3652197	33	Before Sarkadeh	696343	3640348
16	After Shar-e-Amir	682190	3651970	34	After Sarkadeh	696488	3639921
17	Kharvazan River	682069	3652570	35	Dehloran Bridge	702045	3624751
18	Kan-e-Shaloo	700593	3663852				

[DOI: 10.22034/ECOPERSIA.12.3.283]

Four hundred twenty water samples were collected at three points of each cross-section at 35 sampling sites and from different depths. Then, all samples were collected in 1000 ml sterile polypropylene bottles initially prewashed, rinsed with deionized water, and labeled to assess the chemical compositions. Among 14 physio-chemical parameters chosen for measurement, water temperature [24], pH, and electrical conductivity (EC) were measured in situ by a portable multimeter (Waterproof CyberScan PC 300 Portable pH / Conductivity / TDS Meter with pH electrode, EC-FC72522-01B). Also, surface flow velocity was measured in situ using the flow meter (Model 801 – EM the Flow Meter), and then the discharge of flow was estimated using the Mean Section Method [25] (as seen in Eq. (1)).

$$Q=\left(\frac{W_1\times W_2}{2}\right)(V_1D_1)+\left(\frac{W_2\times W_3}{2}\right)(V_2D_2)+\ldots+\left(\frac{W_n\times W_{n+1}}{2}\right)(V_nD_n) \quad \text{Eq.(1)}$$

Where Q refers to discharge ($m^3.s^{-1}$), W is the wide cross-section (m), V is the mean flow velocity ($m.s^{-1}$), and D defines the depth of flow (m).

Total dissolved solids (TDS), Total Hardness (TH), magnesium (Mg^{2+}), sodium (Na^+), calcium (Ca^{2+}), potassium (K^+), chloride (Cl^- [1]), bicarbonate (HCO_3^-), and sulfate (SO_4^{2-}) were determined in the laboratory. Sodium adsorption ratio (SAR) was estimated using Eq. (2) [25].

$$SAR=\frac{Na^+}{\sqrt{0.5\left(Ca^{2+}+Mg^{2+}\right)}} \quad \text{Eq. (2)}$$

Some quality parameters, including Na^+, K^+, Ca^{2+}, Mg^{2+}, Cl—, and SO_4^{2+}, were analyzed using ion chromatography (ICS—1000, Dionex), while HCO_3 was determined by titration. All steps were carried out using standard methods, including sampling, transferring the samples to the laboratory and their preservation processes, and chemical analysis of the surface water parameters [26].

Data Analysis

Missing values, outliers, and random and systematic errors are common in a monitoring program. As an initial data analysis stage, we visually assessed the data sets to identify some inadvertent errors, such as transcription errors. The normal probability plot was also used to screen more subtle errors and outliers.

Then, the various quality metrics were calculated for each station and season to find the mean, maximum, minimum, standard deviation, and coefficient of variation (CV). Using the GIS with Spearman correlation, Principal Component Analysis (PCA), and Agglomerative Hierarchical Clustering (ACA), we assessed the hydrochemical surface-water data acquired to ascertain the water quality. The statistical analysis of the hydrochemical parameters aids in our identification of the primary factors influencing changes in water quality over time [27]. Kolmogorov-Smirnov test was also performed to check the normality of the data prior to statistical analysis [28, 29]. We Used XLSTAT for statistical analysis of the influential factors in the geometric and morphological changes of the river in this study.

1.Based on the results, the association between the variables was measured using the Spearman correlation [30]. The non-parametric Spearman test was computed using Eq. (3).

$$\rho=1-\frac{6\sum d_i^2}{n\left(n^2-1\right)} \quad \text{Eq. (3)}$$

where ρ is the Spearman rank correlation, n defines the number of observations, and di denotes the difference between the ranks of related variables. There is a correlation

[DOI: 10.22034/ECOPERSIA.12.3.283]

between two variables when the coefficients are high. When two variables are positively correlated, there is said to be a similarity between the correlated variables; when they are negatively linked, the variables develop in opposing directions [27]. Then, an Agglomerative Hierarchical Cluster Analysis (HCA) was conducted on the river water data to identify the specific pattern of similar observations among the variables under investigation [1]. Using hierarchy, HCA aims to group observations into subgroups. Since the agglomerative clustering method made it easy to see the river divided into several groups, we used it. In this study, we focused on the agglomerative strategy to spatially and temporally cluster the data as it can simply visualize groups. To calculate the separation between the observations, we employed the Euclidean Distance. Additionally, we decided to combine clusters using the Ward linkage approach [8] since, in contrast to other combination techniques, it allows for considering cluster variance for quantitative variables [31]. Next, to make complex patterns in data matrices more understandable, Principal Component Analysis (PCA) was performed [32]. The PCA is a dimension reduction approach widely used to interpret large datasets. Creating new uncorrelated variables, which are linear combinations of the original variables, PCA reduces the dimensionality of a dataset in an interpretable way while preserving as much information as possible [33]. PCA calculates matrices to project the variables in a new space, using a new matrix showing the degree of similarity between the variables. Bartlett's sphericity test and Kaiser-Meyer-Olkin (KMO) test were used to test the suitability of the data for PCA [34].

Findings

Table 5 briefly includes the mean values, maximum, minimum, and standard deviation [35], and the coefficient of variation (CV) of the 12 water quality parameters measured during the sampling period of one year at 35 sites along the Meymeh River. Table 5 shows a high dispersion (SD and CV) for some variables, such as TDS, EC, Cl^-, Na^+, K^+, Mg^{2+}, and SAR, mostly during autumn. The result also shows that the major ions in water samples have the following order of concentration: $Na^+ > Ca^{2+} > Mg^{2+} > K^+$ and $CL^- > SO_4^{2-} > HCO_3^-$ during the year. The amount of EC, cations, and anions increases in the summer.

Table 6 shows a correlation matrix including all variables' correlation coefficient (r). A correlation coefficient of $r \geq 0.5$ is considered significant (as highlighted in bold in Table 6). The annual mean of Cl^- and Na^+ in the water samples obtained from the Meymeh River changed from 30.43 to 87.25 $mg.L^{-1}$ and 22.37 to 69.83 $mg.L^{-1}$ before and after the confluence with the tributary of the Sarkadeh River (Nos. 33 and 43), respectively.

Figure 3 shows that the value of EC and, consequently, the concentrations of anions and cations were noticeably increased from the source to the downstream of the river. So, the minimum values were recorded at the river sources with the annual mean of 414.9 and 423.5 $\mu s.cm^{-1}$ at the eastern and western springs of the Meymeh River (No. 1 and 2), respectively. The maximum values were measured at the Siyoul station (No. 30) with an annual mean of 77750 $\mu s.cm^{-1}$. As well, the annual means of EC value was 21560 $\mu s.cm^{-1}$ at Ghadah sulfur spring (No. 29). The annual mean of EC, the sum of the concentrations of anions and cations, was 3440.08 $\mu s.cm^{-1}$, 37.8 and 38.02 $mg.L^{-1}$ at the Varazan station (No. 21). These values reached 11029.2 and 14625 $\mu s.cm^{-1}$, 117.66 and 343.09 $mg.L^{-1}$, 117.09 and 273.61 $mg.L^{-1}$ at the Sarkadeh (No. 34) and Dehloran bridge (No. 35) stations, respectively.

Cluster Analysis:

Since a high dispersion of the water quality

[DOI: 10.22034/ECOPERSIA.12.3.283]

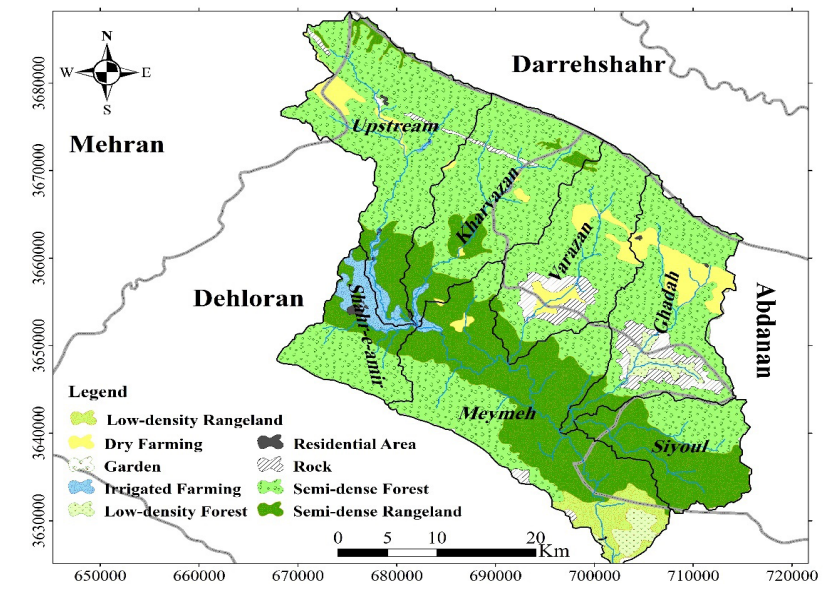

(a) (b)

Figure 2) A scheme of the land uses and sub-watersheds in the Meymeh Watershed, with pictures from the field surveys. (a) refers to the Siyoul salty sub-watershed, where salt deposits are visible on the surface and around the stream; (b) refers to the main river at site 13.

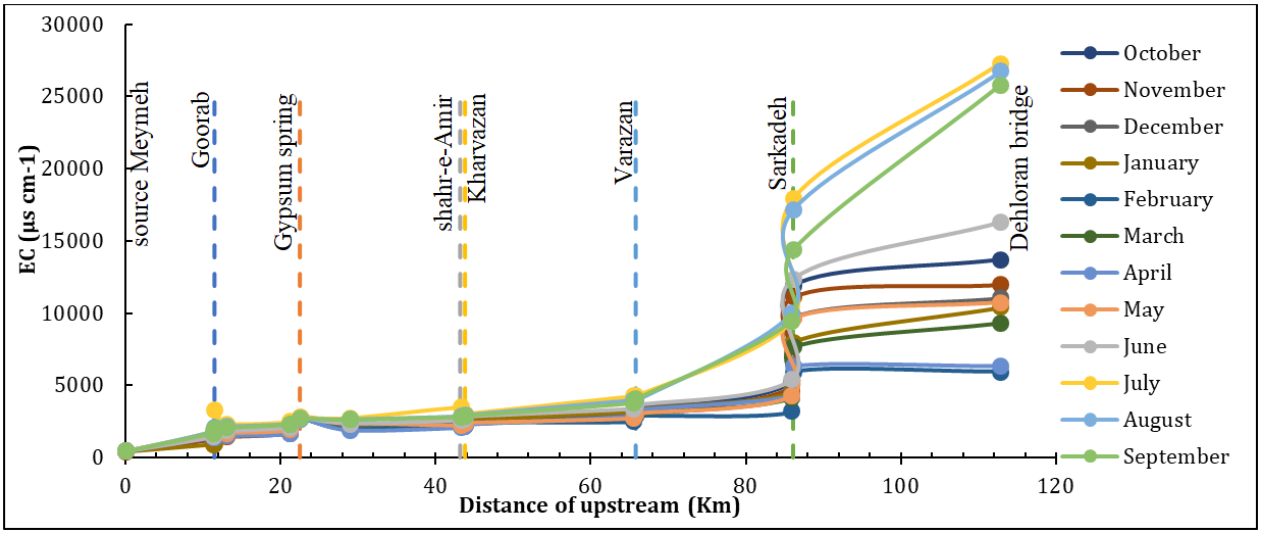

Figure 3) Spatial variations in the electrical conductivity at the confluence of seven tributaries of Goorab, Gypsum Spring, Shahr-e-Amir, Kharvazan, Varazan, Sarkadeh and Dehloran bridge in 12 months from September 2016 to August 2017.

[DOI: 10.22034/ECOPERSIA.12.3.283]

parameters was observed within the seasons, the sampling period (12 months) was divided into three different groups based on their hydrological characteristics using hierarchical cluster analysis (HCA) (Figure. 4). December, January, February, March, April and May were grouped into cluster 1 which closely corresponds to the high flow period (HFP). This period is affected by rainfall events and spring floods. Cluster 2 includes October, November, and June, which approximately relates to the mean flow period (MFP) in the west of Iran. It is the interim between dry and wet seasons. Cluster 3 also includes July, August, and September, corresponding to the low flow period (LFP).

Spatial HCA grouped 35 sampling sites into four district clusters (Figure. 5). Cluster 1 (including Sites 1, 2, 3, 4, 5, 6, 7, 8, 9, 12, 22, and 23) corresponds to a less polluted region. Sites 1, 2, 3, 4, 12, 22, and 23 are upstream.

Cluster 2 (including sites 10, 11, 13, 14, 15, 16, 17, 18, 19, 20, 21, 24, and 26) corresponds to a relatively less polluted region. These sites are mostly in the midstream. Crossing over the formations with high solubility (especially the Gachsaran Formation), water quality in this part gradually decreases from upstream to downstream.

Cluster 3 (including sites 25, 27, 28, 29, 31, 32, 33, 34, and 35) corresponds to a relatively high-polluted region. It includes the sites at the river's outlet, in the Ghadah sub-watershed, and around the sulfur spring. Sites 34 and 35, where the water quality is inferior, are at the watershed outlet after the confluence of the Ghadah and Meymeh Rivers.

Cluster 4 is related to Site 30, at the outlet of the Siyoul sub-watershed, downstream of salty zones (Figure. 6-zone B). This site's hydrological condition differs utterly from other clusters, severely reducing water quality. The hydrogeological conditions of

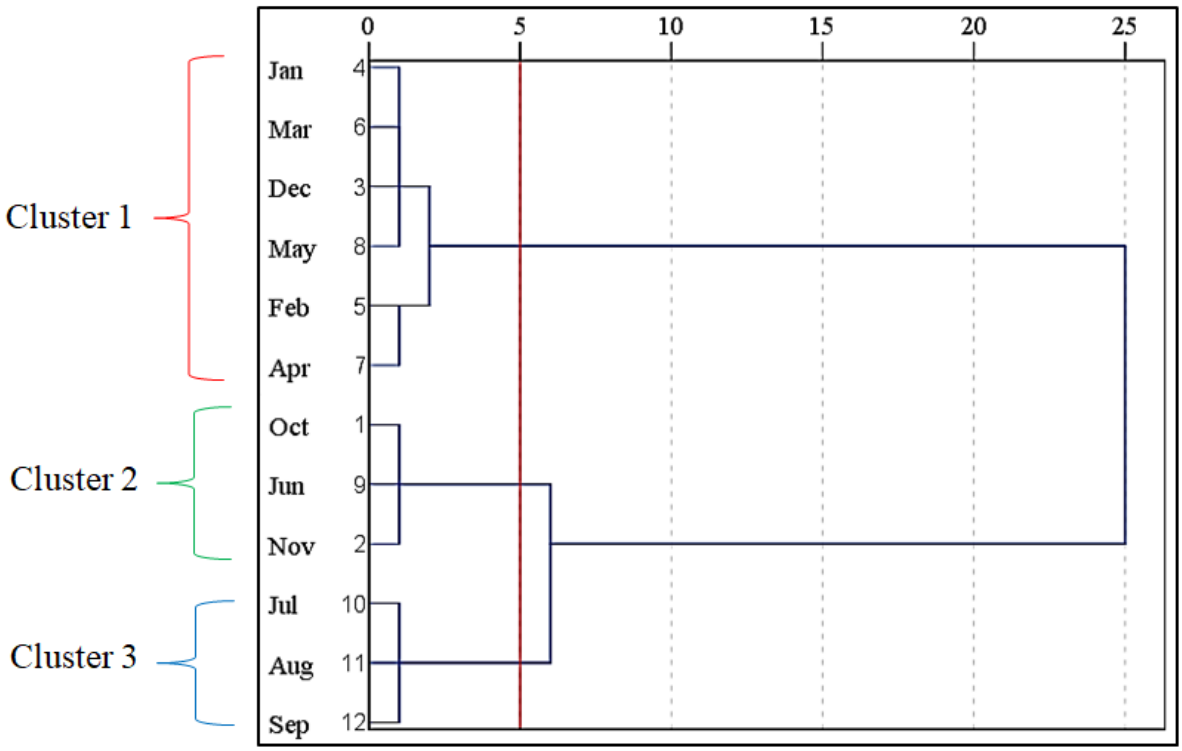

Figure 4) Dendrogram showing clustering of monitoring periods (12 months from September 2016 to August 2017) based on hierarchical clustering, Ward's method.

[DOI: 10.22034/ECOPERSIA.12.3.283]

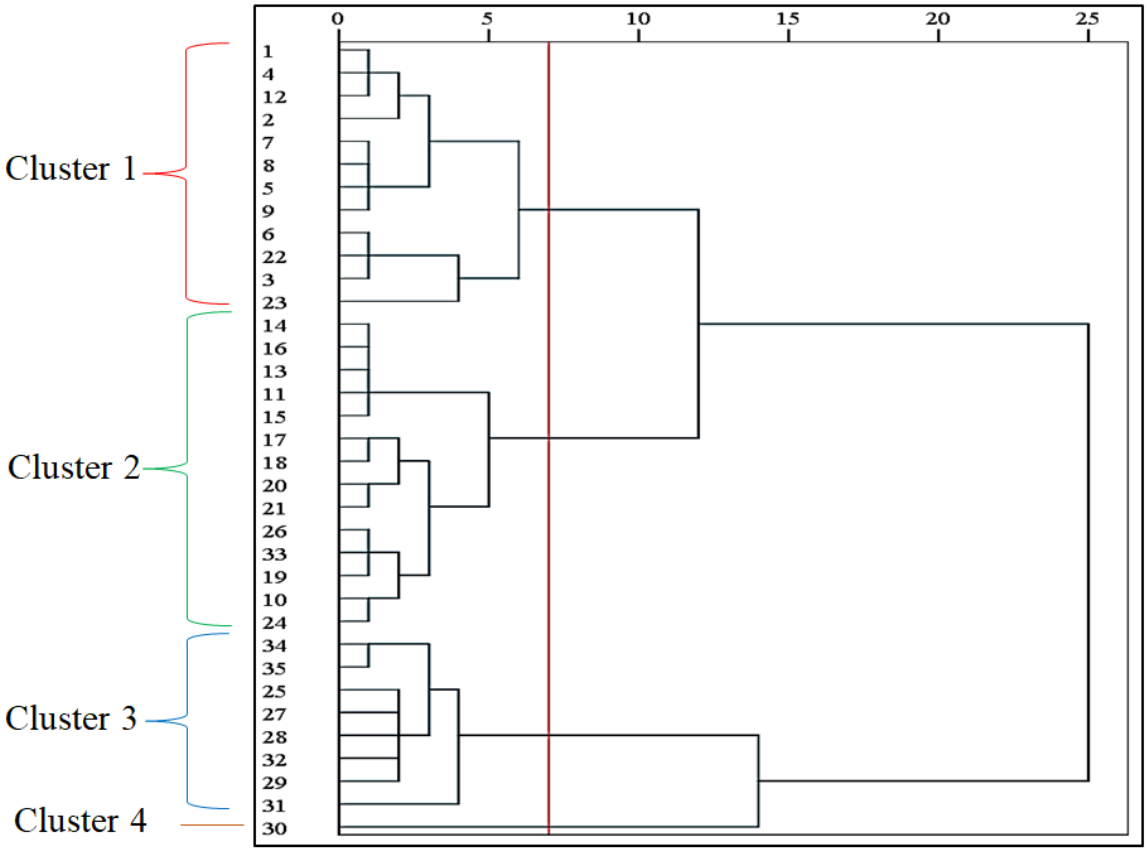

Figure 5) Dendrogram showing clustering of the 35 monitoring sites based on hierarchical clustering, Ward's method.

the Siyoul tributary (before and after salty zones) were recorded in October, January, and July (2016-2017). Based on the results, EC was 4030 $\mu s.cm^{-1}$ in October 2016 before the salty zones. This value reached 34,700 $\mu s.cm^{-1}$ and 122100 $\mu s.cm^{-1}$ immediately after passing the first and second salty zones, respectively. The flow rate was constant along the flow path. So, it can be said that the Gachsaran Formation, with layers of salt, has a significant role in controlling water quality in this area.

Piper Diagrams

We also plotted Piper Trilinear diagrams [9, 50] for samples from different stations to illustrate chemical differences between the various clusters (Figure. 5) and differentiated naturally occurring water and rock interactions (Figure. 7).

According to the analytical results, water samples demonstrated distinct characteristics based on local geology in the study area. Cluster 1, including upstream sites mainly surrounded by the Ilam Formation (Figure. 1), was of the calcium-bicarbonate type. Ilam Formation consists of fine-grained clayey limestones. These limestones have regular stratification and are associated with black shales. Since the solubility of the CO_2 in water increases as the temperature decreases, mountain streams are commonly highly saturated in CO_2 [51]. According to Klimchouk [14], the solubility of calcium carbonate increases in the presence of the CO_2 gas. Hence, the interaction between water saturated with carbon dioxide and limestone increases the chance of dissolving more calcium and bicarbonate upstream of the river. Cluster 2, including midstream sites surrounded mainly by the Gachsaran Formation with the main evaporative minerals of anhydrite, halite, and gypsum, represented Ca^{2+}- SO_4^{2-} dominance.

[DOI: 10.22034/ECOPERSIA.12.3.283]

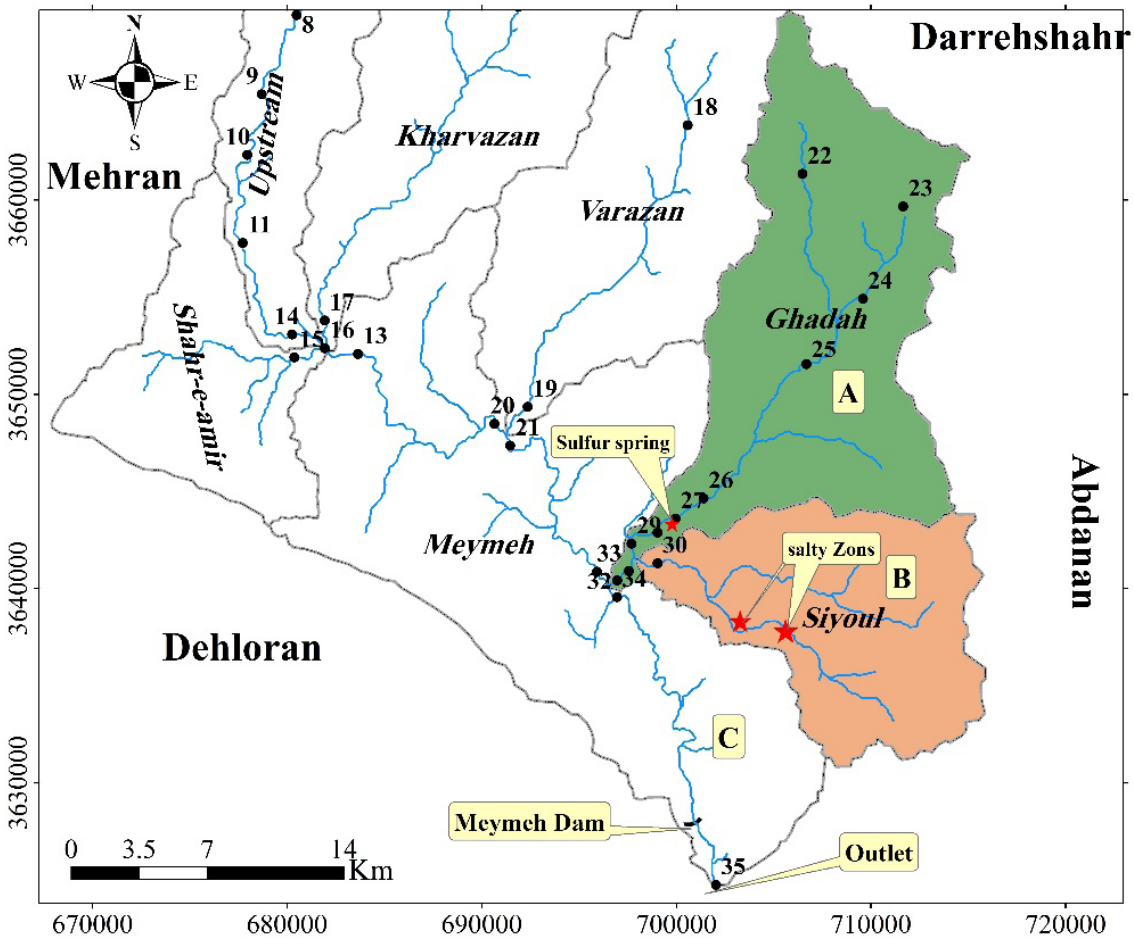

Figure 6) The Ghadah (A) and Siyoul (B) sub-watersheds and the location of the salinity zones and sulfur spring.

Also, the Ghadah and Siyoul streams, which flow around the sulfur spring and salty zones, were found to be enriched with Na^+-Cl^--SO_4^{2-} (Clusters 3 and 4). The natural increase in Cl^- demonstrates the salinization process for water flow in cluster 3 [52]. Moreover, Boulom et al. [53] outlined that the enrichment of Na^+ content in water is due to interaction with salt deposits and probably the ion exchange process. Site 30, at the outlet of the Siyoul sub-watershed, where the stream crosses over the salty zones, is characterized by Na^+– SO_4^{2-} facies. According to Klimchouk [14], waters containing some dissolved salts can influence the solubility of other minerals. The increment in ionic strength and ion pairing can reduce the activities of SO_4^{2-} and result in increased solubility.

Principle Component Analysis (PCA.)

Temporal PCA was further applied to the data sets containing 12 water quality variables at 35 stations, separately for three periods, viz., low (LFP), mean (MFP), and high (HFP) flow periods, extracted from cluster analysis, to compare the temporal pattern of water quality and to identify the factors more influencing them. The sampling adequacy was tested using Kaiser-Meyer-Olkin (KMO) [1]. Besides, Bartlett's test of sphericity was performed to verify that PCA can compress the data meaningfully. The results showed that the KMO for HFP, MFP, and LFP were 0.874, 0.911, and 0.913, respectively, and Bartlett's test was significant (0.000, $p<0.05$), showing that the sampling adequacy was appreciable enough. PCA

[DOI: 10.22034/ECOPERSIA.12.3.283]

Table 5) Descriptive statistics of the 12 physicochemical parameters of water samples measured during the sampling period of one year at 35 sites along the Meymeh River (1).

	Statistics	Q ***	T.D.S*	EC**	pH	HCO_3^{-*}	CL^{-*}	SO_4^{2-*}	Ca^{2+*}	Mg^{2+*}	Na^{+*}	K^{+*}	S	TH*
AR THE* H.F.P.	Mean	1.03	4201.73	6262.91	7.67	3.58	39.36	19.94	23.08	5.38	34.12	0.26	7.95	1405.62
	Max	9.44	46163.00	68900.00	7.98	8.40	601.00	260.20	79.70	48.00	577.30	2.10	254.20	5925.00
	Min	0.00	258.00	404.00	7.18	2.10	0.40	0.30	2.50	0.20	0.32	0.01	0.16	0.67
	SD	1.32	7015.58	10283.28	0.21	0.94	86.72	24.52	14.46	6.89	88.69	0.25	24.58	978.36
	CV%	128.28	166.97	164.19	2.71	26.27	220.31	122.96	62.65	128.04	259.97	94.56	309.11	69.60
MFP	Mean	0.65	5924.74	8610.45	7.60	3.22	57.75	25.93	25.72	6.42	54.69	0.38	30.06	1612.13
	Max	2.70	65928.00	98400.00	7.99	7.00	920.00	526.70	86.00	51.70	865.40	11.07	1007.00	5850.00
	Min	0.00	253.00	396.00	7.01	1.80	0.30	0.20	2.60	0.20	0.30	0.01	0.18	140.00
	SD	0.74	11174.98	16531.29	0.29	0.93	135.18	54.30	16.85	9.25	145.69	1.16	143.22	1183.07
	CV%	112.28	188.62	191.99	3.82	28.98	234.09	209.40	65.54	144.17	266.37	304.95	476.43	73.39
LFP	Mean	0.17	7411.27	11010.84	7.68	3.40	111.78	27.98	33.09	7.93	102.14	0.35	24.29	2018.02
	Max	0.64	81606	121800	7.99	8	2300	67.60	106.40	53	2214	1.51	124.44	6950
	Min	0.00	260	407	7.12	2	0.30	0.22	3.90	0.70	0.42	0.01	0.28	23.25
	SD	0.16	13542.84	20192.99	0.23	1.09	293.05	14.67	20.40	9.09	279.38	0.27	30.42	1376.99
	CV%	90.04	182.73	183.39	3.01	32.03	262.17	52.42	61.65	114.56	273.52	77.99	125.23	68.23
	WHO[1]		500	1500	6.5-8.5	500	250	250	75	50	200	12	-	500

* mg. L^{-1} **µs.cm^{-1} ***m^3. s^{-1}

Table 6) Correlation matrix of the 12 physico-chemical factors of water samples measured at 35 sites in the Meymeh River (Bold numbers indicate significant correlation (r ≥ 0.5).

Variables	Q	TDS	EC	PH	HCO_3^-	CL^-	SO_4^{2-}	Ca^{2+}	Mg^{2+}	Na^+	K^+	SAR	TH.
Q	**1.00**												
TDS	-0.01	**1.00**											
EC	-0.01	**1.00**	**1.00**										
PH	0.08	-0.02	-0.02	**1.00**									
HCO_3^-	-0.07	-0.48	-0.48	-0.12	**1.00**								
CL^-	0.05	**0.96**	**0.96**	-0.01	-0.43	**1.00**							
SO_4^{2-}	-0.12	**0.82**	**0.82**	0.00	**-0.52**	**0.75**	**1.00**						
Ca^{2+}	-0.09	**0.96**	**0.96**	-0.03	-0.48	**0.92**	**0.85**	**1.00**					
Mg^{2+}	-0.04	**0.85**	**0.85**	0.01	-0.36	**0.82**	**0.70**	**0.79**	**1.00**				
Na^+	0.04	**0.93**	**0.93**	0.00	-0.44	**0.91**	**0.76**	**0.88**	**0.79**	**1.00**			
K^+	-0.03	**0.80**	**0.81**	-0.05	-0.29	**0.78**	**0.70**	**0.82**	**0.68**	**0.75**	**1.00**		
S.A.R.	-0.06	**0.73**	**0.73**	0.06	-0.30	**0.69**	**0.62**	**0.72**	**0.67**	**0.83**	**0.61**	**1.00**	
TH	-0.06	**0.95**	**0.95**	0.00	-0.47	**0.91**	**0.81**	**0.94**	**0.84**	**0.87**	**0.78**	**0.71**	**1.00**

[DOI: 10.22034/ECOPERSIA.12.3.283]

could be considered an efficient technique that can significantly reduce the data set. The datasets were compressed into fewer uncorrelated factors by interpreting the correlation matrix [45]. Using PCA, which extracts 2 PCs with eigenvalues>1, explaining 86.81, 90.21, and 91.32 (%) of the total variance for HFP, MFP, and LFP, respectively (Table 7).

The contribution of the original variables in the new factors produced by PCA, separately for three periods, viz. HFP, MFP, and LFP are presented in Figure 8 (a). As observed in the result, PC1 has strong positive loadings on E.C., T.D.S., Cl^-, SO_4^{2-}, Ca^{2+}, Mg^{2+}, Na^+, K^+, S.A.R. and total hardness, while correlates negatively with HCO_3^- in H.F.P. and L.F.P. (79.2 and 82.46 (%) of total variance, respectively). PC2 strongly correlates with pH in HFP and LFP (7.61 and 8.86 (%) of the total variance, respectively). PC3 also positively loads HCO_3^- in MFP (6.36 (%) of total variance). Also, factor scores related to PC1 and PC2 comprised four surface water groups in HFP and LFP (Figure. 8 b).

Discussion

Based on the results, a high dispersion (SD and CV) is seen for some variables, such as TDS, EC, Cl^-, Na^+, K^+, Mg^{2+}, and SAR, mostly during autumn. According to Zeinalzadeh and Rezaei [36], the magnitude of water quality changes depends on system-specific watershed characteristics, river regimes, and human activities. The chemical composition of water temporally changes at the end of the seasons, especially in autumn, which increases the amount of rainfall and significantly increases the river's flow rate. The decline in water quality has sped up from the Meymeh station (No. 9, Figure. 1) in response to geological restructuring. The peak concentration of elements was observed at the confluence of the Siyoul and Sarkadeh tributaries to the Meymeh River (No.34), where the salt layers in the Gachsaran Formation are exposed. A strong positive correlation was found between EC, Cl^-, SO_4^{2-} and cations. In a comparable study, Varol et al. [8] investigated the spatial and temporal variations in surface water quality in the Tigris River Basin, Turkey. They also observed a high positive correlation between EC, TH, SO_4^{2-}, Na^+, and Ca^+ (r=0.547 to 0.886), which are responsible for water mineralization.

The positive and high coefficient between TDS and the other elements (Cl^-, SO_4^{2-} and cations) was detected. However, a mild negative correlation was observed between the flow rate and almost all the significant elements and EC since an increase in flow rate caused the dilution of contaminants [38]. Besides, negative correlation coefficients were measured between HCO_3^- and Ca^{2+}, Mg^{2+}, SO_4^{2-} and TDS (Table 6). Generally, if the pH of water remains constant, Ca^{2+} and HCO_3^- are negatively correlated, which implies that the increase in bicarbonate ions will decrease the solubility of Ca^{2+} [39].

The annual mean of Cl^- and Na^+ was

Table 7) Eigenvalues and explained variance of 12 water quality variables at 35 stations in three HFP, MFP, and LFP periods.

	HFP		MFP		LFP	
	PC1	PC2	PC3	PC4	PC5	PC6
Eigenvalue	1.004	0.913	9.776	1.050	9.895	1.063
Variability (%)	79.202	7.612	81.466	8.751	82.462	8.861
Cumulative %	79.202	86.814	81.466	90.217	82.462	91.322

[DOI: 10.22034/ECOPERSIA.12.3.283]

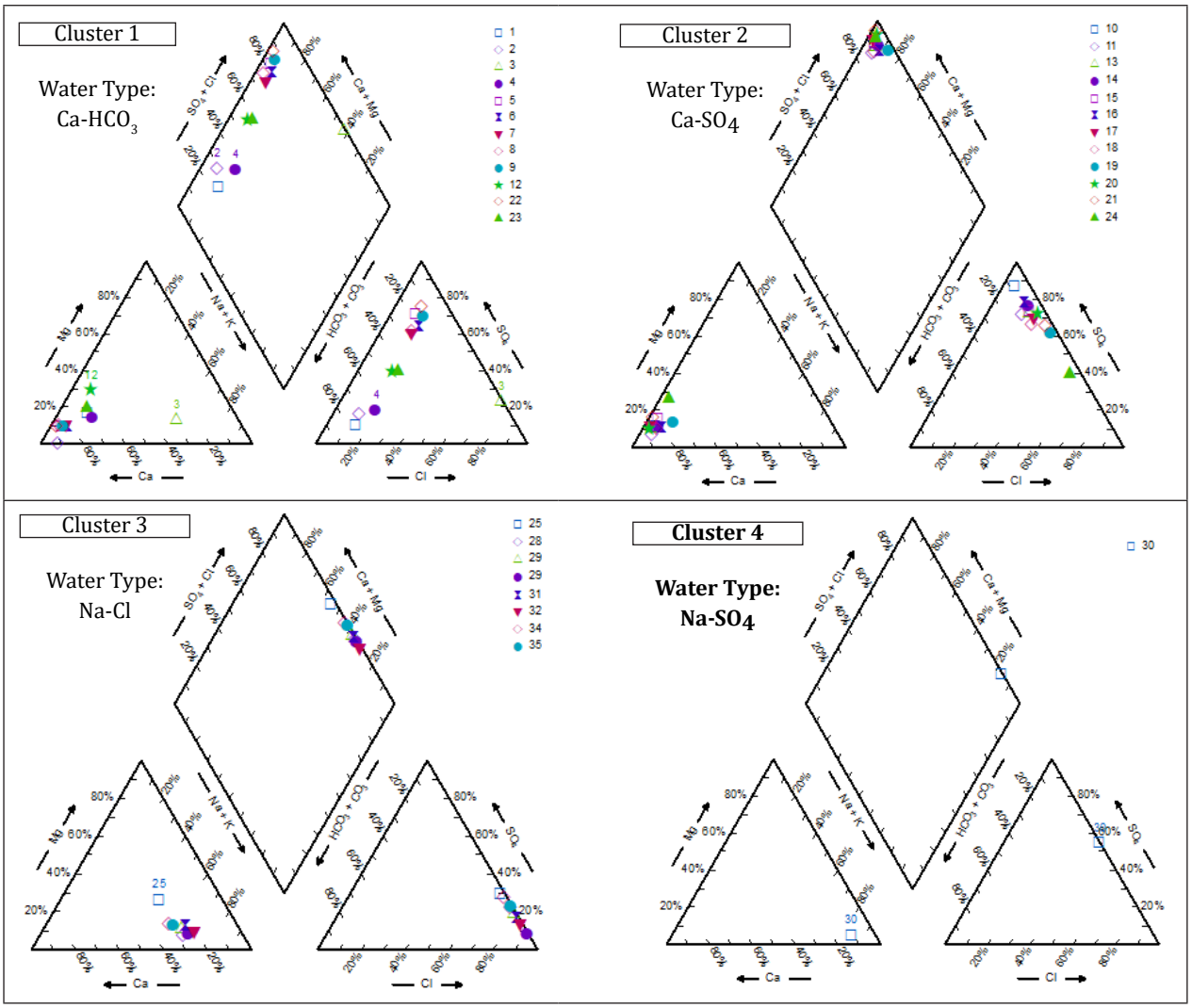

Figure 7) Piper trilinear diagrams showing dominant cation and anion fields in the Lower triangles and the water types in the upper diamond (using Rockware AqQA software).

considerably increased before and after the confluence with the tributary of the Sarkadeh River (No.33 and 43). So, the sudden increase in the concentrations of elements from the confluence of the Sarkadeh River to the Meymeh River indicates that salt dissolution is the main factor in reducing the water quality of the Meymeh River. The source of this salt is a salt accumulation in the Gachsaran Formation, especially in its lower parts, which have approached the earth's surface because of the geological structure along the Siyoul and Ghadah tributaries. An example is a salt mine in the southwest of the study area from which the ancient people got their salt.

According to the results, a slight increase was observed in sulfate, calcium, and magnesium concentrations from the upstream to the downstream of the Meymeh River due to the dissolution of gypsum along the river. The bicarbonate ion was almost constant, with a mild downward trend from the upstream to the downstream due to the release of some carbon dioxide in the water due to water flow along the river path. Scrutiny in the sodium and chlorine concentrations showed that they followed the same pattern in changes with EC. The sudden increase in their concentrations after the confluence of the Sarkadeh and Meymeh Rivers emphasized the fact that salt dissolution was the main

[DOI: 10.22034/ECOPERSIA.12.3.283]

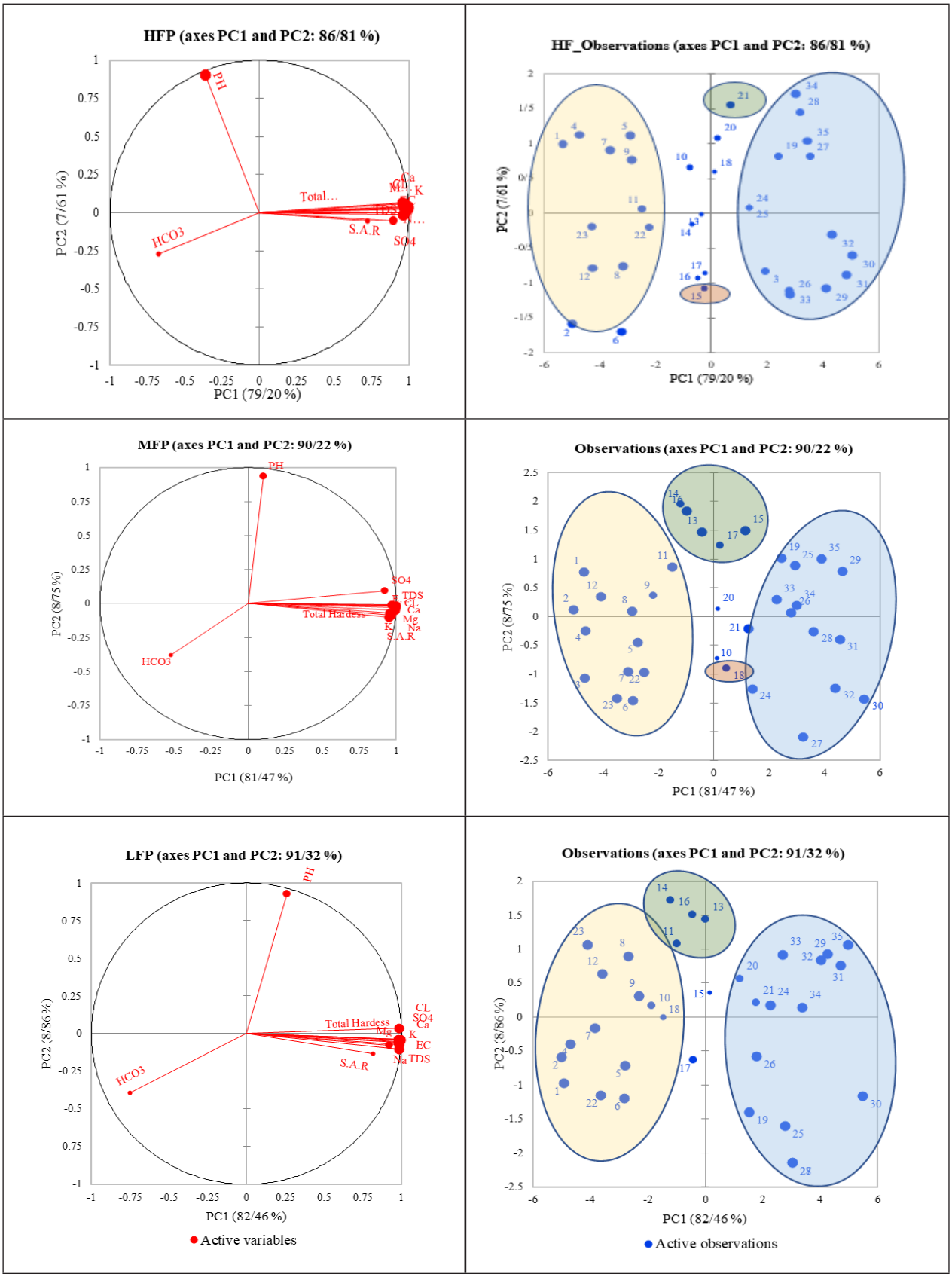

Figure 8) Factor loadings of 12 water quality variables (a1-a3) and Factor scores for 136 observations at 35 stations (b1-b3) in the coordinates of the first two principal components. Numbers refer to the code of each sampling site.

[DOI: 10.22034/ECOPERSIA.12.3.283]

factor in reducing the quality of the Meymeh River (Figure. 3). Field surveys revealed that the water quality of the Meymeh River decreases gradually by passing through the evaporative formations.

Also, a slight downward trend in water salinity was observed over a distance of about four kilometers between two stations of Nos. 31 and 32. The reason may refer to high evaporation in that area, which leads to salt depositions in the river bed.

According to the results, the quality of the Sarkadeh River drastically decreases where the Siyoul tributary and sulfur spring (No 29 in Figure. 1) feed the river. Higher water temperature compared to the other parts of the river and the strong sulfur odor near the sulfur spring can point out the possibility of a fault and deep-water cycles underground. According to the field surveys, the water sinks into the ground around the sulfur spring and some parts of the Gachsaran Formation and does not reappear downstream.

The annual mean of EC at the Sarkadeh station (No. 33) was recorded at about 27000 $\mu s.cm^{-1}$, in September (LFP). This value reached 11000 $\mu s.cm^{-1}$ after flowing into the Meymeh River. Along with Zeinalzadeh and Rezaei [36], Zhang et al. [40] and KurunÇ et al. [41] it was expected to observe a higher concentration of EC during LFP. It should be noticed that the amount of this parameter decreased significantly during the high-flow period due to the dilution of river water (e.g., the EC amount was measured at about 2400 $\mu s.cm^{-1}$ downstream (No. 35) two days after a flood event in February). So, it can be said that the Sarkadeh River is the main factor in reducing the water quality of the Meymeh River. Accordingly, the status of the Siyoul tributary and the sulfur spring (tributaries of the Sarkadeh River) were examined separately.

The base flow is very low in mainstreams, and most source tributaries are dry in LFP. Correspondingly, the concentration of water-soluble elements is relatively high (Figure. 4). Zhang et al. [40] also reported that reduced river flows, increased pollution values, and agricultural drainage water depletions have caused a critical situation in river quality. This temporal similarity pattern is more reasonable for understanding the study area better, as it fits more with the climate condition of the region rather than the four normal seasons.

Spatial HCA grouped the sampling sites into four district clusters (Figure. 5). All clusters correspond to low/high polluted regions, confirmed by their spatial characterization and consistent with the result using water quality parameters. Ejaz [42], Varol [8], and Simeonov et al. [37] also confirmed that the CA technique was suitable for offering a reliable classification of surface waters in the whole catchment.

According to the P.C.A. results, PC1 has strong positive loadings on E.C., T.D.S., Cl^-, SO_4^{2-}, Ca^{2+}, Mg^{2+}, Na^+, K^+, S.A.R. and total hardness. In other words, PC1 represents river water mineralization. Comparing the results and the geology map, this factor exhibits the importance of water-rock interaction processes in the watershed. PC2 provides a strong positive correlation with pH in HFP, and LFP PC3 also has positive loading on HCO_3^- in MFP (Figure. 8a).

Factor scores comprised four surface water groups in HFP and LFP (Figure. 8 b). Group 1 in HFP has a negative correlation with PC1 and mostly represents samples from the source of tributaries during HFP (sites 1, 2, 4, 5, 6, 7, 8, 9, 11, 12, 22, and 23). This group is characterized by relatively low E.C., T.D.S., Cl^-, SO_4^{2-}, Ca^{2+}, Mg^{2+}, Na^+, K^+, S.A.R. and total hardness, and high HCO_3^-. Group 2 positively correlates with PC1 and mostly involves samples from downstream (site 3, 19, 24, 25, 26, 27, 28, 29, 30, 31, 32, 33,

[DOI: 10.22034/ECOPERSIA.12.3.283]

34 and 35). This group is characterized by relatively high E.C., T.D.S., Cl^-, SO_4^{2-}, Ca^{2+}, Mg^{2+}, Na^+, K^+, S.A.R. and total hardness, and low HCO_3^-. Group 3 and Group 4 (15 and 21) also represent an intermediate chemical composition between Group 1 and Group 2. They are mostly characterized by pH. Mixing water between groups (sites 10, 13, 14, 16, 17, 18 and 20) represents an intermediate chemical composition.

Group 1 in MFP shows a negative correlation with PC1. This group can be described by comparatively low EC, TDS, Cl^-, SO_4^{2-}, Ca^{2+}, Mg^{2+}, Na^+, K^+, SAR, and total hardness and high HCO_3^- and represent samples from the sites 1, 2, 3, 4, 5, 6, 7, 8, 9, 11, 12, 22 and 23. Group 2 refers to sites 19, 21, 24, 25, 26, 27, 28, 29, 30, 31, 32, 33, 34 and 35 which show a positive correlation with PC1. This group is also characterized by high E.C., T.D.S., Cl^-, SO_4^{2-}, Ca^{2+}, Mg^{2+}, Na^+, K^+, S.A.R. and total hardness, and low HCO_3^-. Group 3 (site 18) and Group 4 (sites 13, 14, 15, 16, and 17) are mostly characterized by pH during MFP. LFP also follows a similar pattern to HFP, with slight differences in the middle parts of the river.

In comparable studies, Zeinalzadeh and Rezaei [36] and Ouyang et al. [43] indicated that the main quality parameters affecting the river quality of each river could be different from other rivers. It can also be unique for each river and vary along the stream. The reason can be found in different environmental statuses, climatic conditions, and human activities around the river. In other words, contaminants affecting river water quality have temporal and spatial variations and should be considered based on each climatic and river's conditions. Olsen et al. [44] concluded that principal components and scores could be used to explore further spatial patterns in the comprehensive water quality of watersheds affected by runoff/infiltration from upstream of the watershed.

Conclusion

Investigation of the relationship between electrical conductivity and water-soluble ions along the Meymeh River shows that bicarbonate ions are almost constant along the path. However, a downward trend is observed in some parts of the river, possibly due to the release of some carbon dioxide from the water into the atmosphere. There is a slight increase in sulfate, calcium, and magnesium ions because of the dissolution of gypsum along the river. The water quality of the Varazan River (downstream of the Meymeh River- site 19) is considerably characterized by the presence of salt springs. However, this decline in quality peaks at once at the confluence of the Sarkadeh tributary with the Meymeh River (site 33). The main factors reducing the quality of the Sarkadeh tributary are the Ghadah sulfur spring (site 29 upstream of the Sarkadeh River) and the Siyoul tributary, which passes through two salinity zones before flowing into the mainstream. The Siyoul River enters a ponor within the first salinity zone and gradually emerges at about 150 to 200 meters from the sediments. In the second salinity zone, the water gradually disappears in an area at the bottom of the river and reappears at about 200 meters, seeping out of sediments. The sulfur spring is located along the Ghadah River and upstream of the confluence of the Siyoul and Sarkadeh tributaries, which has a mean annual flow of about 300 l. s^{-1} and a mean EC of 21590 µs.cm^{-1} (site 29) significantly contributes to reducing the quality of the Sarkadeh tributary. Considering the laboratory results of the experimental samples, the EC value increased about 3.5 times in Site 27, compared to its upstream by the entrance of the water of the sulfur spring. The salinization of this spring mainly relates to the presence of salts in the Gachsaran Formation, especially the salt horizons. The presence of sulfur compounds

[DOI: 10.22034/ECOPERSIA.12.3.283]

(pungent odor of hydrogen sulfide) and its higher temperature than other water sources in the region show the deep rotation of water and the possibility of a fault in these areas. Also, severe folding and crushing of gypsum layers at the source of the spring are pretty visible. Field surveys showed that some waterways have sunk into the ground around the Ghadah sulfur spring and inside the Gachsaran Formation. On the other hand, due to the higher altitude of these points compared to the sulfur spring, there is a potential for the movement of these waters towards the Ghadah sulfur spring. In addition, many sinkholes inside the Gachsaran Formation in the region and the possibility of passing a global fault on the southern slope cause water transfer to sulfur springs. The sudden increase in the amount of sodium and chlorine ions and the high correlation of their changes with the amount of electrical conductivity from the confluence of the Sarkadeh tributary to the Meymeh River indicate that salt dissolution is the main factor in the sudden decline in the quality of the Meymeh River after the Sarkadeh intersection. The source of this salt relates to the salt layers of the Gachsaran Formation, which have approached the surface because of structural reasons along the Siyoul and Ghadah tributaries. These findings are consistent with research results by other researchers such as [46,50]. According to the results, downstream saline springs, the Ghadah sulfur spring, the Siyoul tributary, saline springs inside the reservoir of the dam, and the gradual change by the Gachsaran Formation, respectively 12, 28, 21, 10 and 25 (%) are involved in the salinity of the Meymeh River. As seen, the shares of Ghadah sulfur springs and the Siyoul tributary in reducing the water quality of the Meymeh River are 28 and 21 (%), respectively. In other words, about 50 (%) of the salinity of the Meymeh River is because of the influence of the Sarkadeh River (which results from the combination of the Siyoul River and the Ghadah sulfur spring). Therefore, the factors that reduce the water quality of the Meymeh River are as follows.

1) Dissolution of gypsum of the Gachsaran Formation
2) Saline springs downstream of the Varazan River
3) Ghadah sulfur spring with a mean annual electrical conductivity of 21,600 $\mu s.cm^{-1}$ and a mean flow rate of 0.3 $m^3.s^{-1}$
4) The Siyoul branch with a mean annual electrical conductivity of 77,750 $\mu s.cm^{-1}$
5) Saline springs at the bed and the banks at the site of the dam reservoir.

With the range of different salinity sources in the dam catchment, there are opportunities to manage, reduce, or avoid this salinity. Low-quality water may be diverted around the dam, while high-quality flows experienced after the break of the season may be allowed to enter the dam, e.g., if the sulfur spring is removed or rerouted, the EC value of Ghadah River will decrease from 15971 to 4562 $\mu s.cm^{-1}$. It should be noted that several small springs of salinity and sulfur discharged into the reservoir at the river bed and banks were discovered, which notably contributed to reducing the river's water quality after Sarkadeh's confluence. Since these springs are below the reservoir's normal level, it seems there is no way to prevent the water of these springs from entering the reservoir. However, identifying their origin may be effective in controlling and managing them. To solve the problem in the Siyoul tributary, it is possible to construct a canal in the area where water infiltrates the riverbed in the Gachsaran Formation and reappears. Thus, water can be transferred from the Siyoul tributary downstream of the sinking zone through this canal to prevent it from contacting the salts of the Gachsaran Formation and reducing water quality. In

[DOI: 10.22034/ECOPERSIA.12.3.283]

order to eliminate the input of sulfur to the mainstream, it is necessary to transfer the sulfur water of the Ghadah spring.

Due to the morphology of the river and its flooding, the transfer of the spring water downstream of the dam is only possible through pipes and a suitable bed at the source. Here, the river's salinity can be reduced by up to 50 (%). We also estimated that the electrical conductivity of the Meymeh River will decrease from 12,500 µs.cm $^{-1}$ to 5,700 µs.cm $^{-1}$ before reaching the dam reservoir. It is worth noticing that these estimations were based on the base flow rate of the river (2017-2018), which is considered a dry year. However, considering the annual floods in this area, the electrical conductivity of the reservoir will reach about 5200 to 5300 µs.cm^{-1}. Additional hydrogeological studies and monitoring around the saline springs are strongly recommended.

In conclusion, we can summarize the obtained results as follows.

1- The field surveys and measurements found that river water quality decreases along the river (EC changes from 500 µs.cm^{-1} at the river's source to 12500 at the last station, downstream of the river).

2- Crossing over the saline evaporative formation with high solubility (especially the Gachsaran Formation), water quality gradually decreases upstream to downstream. So, EC reaches 3500 µs.cm^{-1} at the confluence of the Varazan and Kharvazan tributaries).

3- The sulfur spring in the Ghadah River contributes significantly to reducing the quality of the Sarkadeh tributary.

4- Saline springs, Ghadah sulfur spring, the Siyoul tributary, saline springs inside the dam's reservoir, and the gradual change by the Gachsaran Formation, respectively 12, 28, 21, 10, and 25 (%), are involved in the salinity of the Meymeh River.

5- About 50 (%) of the Meymeh River's salinity is due to the influence of the Siyoul River and the Ghadah sulfur spring.

The results provide recommendations for future research. These recommendations can be a basis for future research in water resources management and environmental conservation in the Meymeh River and similar areas.

1- Conducting long-term monitoring studies to investigate changes in water quality and the affecting factors over time. Here, temporal patterns in water quality and seasonal or annual effects will be identified.

2- Evaluating the effectiveness of water resource management strategies. This goal will be possible by implementing the proposed management strategies (such as controlling the entry of salty water) and evaluating their results by regular monitoring.

3- Analysis of the effects of climate change to investigate the impact of climate change on the water quality and quantity of Mime River. The result that can be expected from this study is a better understanding of how climate change affects water resources and providing adopting solutions.

Acknowledgment

The authors are grateful to the Ilam Regional Water Company staff, who has provided the credit for this research in the form of a research plan, also from the laboratory experts of the regional water company, and all colleagues who have cooperated in any way in conducting this study.

Ethical permission: The authors certify that this manuscript is original and that any use of others' work or words has been appropriately cited.

Authors' contributions: The authors of this article cooperated during library studies, field monitoring and sampling, analysis of samples and obtained data, analysis of

[DOI: 10.22034/ECOPERSIA.12.3.283]

results, and compilation of the article.

Funding/ Support: This study was conducted under a memorandum of cooperation between Ilam Regional Water Company and Ilam University.

Conflict of interest: The authors have no conflicts of interest to express consideration for the publication of this paper. They confirmed that co-authors have consented to and are fully aware of the submission.

References

1. Abdollahi Z., Kavian A., Sadeghi S.H.R., Khosrovyan A., DelValls A. Identifying environmental risk associated with anthropogenic activities in Zanjanrud River, Iran, using an integrated approach. Catena. 2019; 183:104156.
2. Faye C. Water Resources and Their Management in an Increasing Urban Demography: The Case of Dakar City in Senegal. Resour. Water 2021:101.
3. Mainali J., Chang H. Landscape and anthropogenic factors affecting spatial patterns of water quality trends in a large river basin, South Korea. J. Hydrol. 2018; 564:26-40.
4. Wijesiri B., Deilami K., Goonetilleke A. Evaluating the relationship between temporal changes in land use and resulting water quality. Environ. Pollut. 2018; 234:480-486.
5. Leonardo Mena-Rivera V.S.-S., Cristina Benavides-Benavides, Juana Coto-Campos, Thomas Swinscoe. Spatial and Seasonal Surface Water Quality Assessment in a Tropical Urban Catchment: Burío River, Costa Rica. Water 2017; 9(8):558.
6. Sahraei Parizi H., Samani N. Geochemical evolution and quality assessment of water resources in the Sarcheshmeh copper mine area (Iran) using multivariate statistical techniques. Environ. Earth. Sci. 2012; 69(5):1699-1718.
7. Barzegar R., Asghari Moghaddam A., Soltani S., Baomid N., Tziritis E., Adamowski J., Inam A. Natural and anthropogenic origins of selected trace elements in the surface waters of Tabriz area, Iran. Environ. Earth. Sci. 2019; 78(8):1-12.
8. Varol M., Gökot B., Bekleyen A., Şen B. Spatial and temporal variations in surface water quality of the dam reservoirs in the Tigris River basin, Turkey. Catena. 2012; 92:11-21.
9. Baba A., Gündüz O. Effect of geogenic factors on water quality and its relation to human health around Mount Ida, Turkey. Water. 2017; 9(1):66.
10. Kavian A., Dodangeh S., Abdollahi Z. Annual suspended sediment concentration frequency analysis in Sefidroud basin, Iran. MESE 2016; 2(1):1-10.
11. Nouri J., Mahvi A., Jahed G., Babaei AJEG Regional distribution pattern of groundwater heavy metals resulting from agricultural activities. Environ. Geol. 2008; 55(6):1337-1343.
12. Khadivi S. Tectonic evolution and growth of the Zagros Mountain Belt (Fars, Iran): constraints from magnetostratigraphy, sedimentology, and low-temperature thermochronometry: Université Pierre et Marie Curie-Paris VI; 2010.
13. Rezaee P., Salari S. Petrography and mineralogy of Gachsaran formation in the west of Bandar-e-Abbas, Kuh-e-Namaki Khamir section, south of Iran. J. Fundam. Appl. Sci. 2016; 8(2):956-969.
14. Klimchouk A. The dissolution and conversion of gypsum and anhydrite. INT. J. S.P.E.L.E.O.L. 1996; 25(3):2.
15. Reiss A.G., Gavrieli I., Rosenberg Y.O., Reznik I.J., Luttge A., Emmanuel S., Ganor J. Gypsum precipitation under saline conditions: thermodynamics, kinetics, morphology, and size distribution. Minerals. 2021; 11(2):141.
16. Ghadiri A., Hashemi S.H., Nasrabadi T. The efficiency of Iran's water resources quality index in comparison with three indices for assessment of Heavy Metal pollution in surface water (Case study: north and east of Tehran's runoff). MCEJ 2021; 21(2):177-188.
17. Shafiee M., Azizipour M., Sasani H., Takdastan A. Assessment of Water Quality in the Karun River of Ahvaz City According to Existing Standards. MCEJ. 2024; 24(1):113-125.
18. López-López J.A., Mendiguchía C., García-Vargas M., Moreno C. Multi-way analysis for decadal pollution trends assessment: The Guadalquivir River estuary as a case study. Chemosphere. 2014; 111:47-54.
19. Ma X., Wang L., Yang H., Li N., Gong C. Spatiotemporal Analysis of Water Quality Using Multivariate Statistical Techniques and the Water Quality Identification Index for the Qinhuai River Basin, East China. Water. 2020; 12(10):2764.
20. Melland A.R., Fenton O., Jordan P. Effects of agricultural land management changes on surface water quality: A review of mesoscale catchment research. Environ. Sci. Policy. 2018; 84:19-25.
21. Mostafaei A. Application of Multivariate Statistical Methods and Water-Quality Index to Evaluation of Water Quality in the Kashkan River. Environ. Manage. 2014; 53(4):865-881.
22. Qian Y., Migliaccio K.W., Wan Y., Li Y. Surface water quality evaluation using multivariate methods and a new water quality index in the Indian River Lagoon, Florida. Water. Resour. Res. 2007; 43(8).

[DOI: 10.22034/ECOPERSIA.12.3.283]

23. Barakat A., El Baghdadi M., Rais J., Aghezzaf B., Slassi M. Assessment of spatial and seasonal water quality variation of Oum Er Rbia River (Morocco) using multivariate statistical techniques. ISWCR 2016; 4(4):284-292.
24. Khan M.Y.A., Gani K.M., Chakrapani G.J. Assessment of surface water quality and its spatial variation. A case study of Ramganga River, Ganga Basin, India. Arab. J. Geosci. 2016; 9(1):1-9.
25. Grzywna A., Bronowicka-Mielniczuk U. Spatial and Temporal Variability of Water Quality in the Bystrzyca River Basin, Poland. Water 2020; 12(1):190.
26. Tokatli C. Water Quality Assessment of Ergene River Basin Using Multivariate Statistical Analysis. LimnoFish. 2020:38-46.
27. Custodio M., Peñaloza R. Data on the spatial and temporal variability of physical-chemical water quality indicators of the Cunas River, Peru. C.D.C. 2021; 33:100672.
28. Walls S., Binns A.D., Levison J., MacRitchie S. Prediction of actual evapotranspiration by artificial neural network models using data from a Bowen ratio energy balance station. Neural Comput. Appl. 2020; 32:14001-14018.
29. Ahmed N., Howlader N., Hoque M.A.-A., Pradhan B. Coastal erosion vulnerability assessment along the eastern coast of Bangladesh using geospatial techniques. Ocean Coast. Manage. 2021; 199:105408.
30. Mahdavi M. Applied Hydrology. Tehran University Press (In Persian) 2007; Vol.1:342.
31. Apha A. WEF (2005) Standard Methods for the Examination of Water and Wastewater, American Public Health Association, American Water Works Association, and Water Environment Federation. Washington, DC. 2007.
32. Feizizadeh B., Abdollahi Z., Shokati B. A GIS-based spatiotemporal impact assessment of droughts in the hyper-saline Urmia Lake Basin on the hydro-geochemical quality of nearby aquifers. Remote. Sens. 2022; 14(11):2516.
33. Varol MJEP Spatio-temporal changes in surface water quality and sediment phosphorus content of a large reservoir in Turkey. Environ. Pollut. 2020; 259:113860.
34. Wang X., Li J., Chen J., Cui L., Li W., Gao X., Liu Z. Water quality criteria of total ammonia nitrogen (TAN) and un-ionized ammonia (NH3-N) and their ecological risk in the Liao River, China. Chemosphere 2020; 243:125328.
35. Liu M., Wang H.-J., Wang H.-Z., Ma S.-N., Yu Q., Uddin K.B., Li Y., Hollander J., Jeppesen E. Decreasing toxicity of un-ionized ammonia on the gastropod Bellamya aeruginosa when moving from laboratory to field scale. Ecotox. Environ. Safe. 2021; 227:112933.
36. Kim M., Jang G.-J., Kim J.-H., Lee M. Speaker Adaptation Using i-Vector Based Clustering. Systems. TIIS 2020; 14(7):2785-2799.
37. Bhat S.A., Meraj G., Yaseen S., Pandit A.K. Statistical assessment of water quality parameters for pollution source identification in Sukhnag stream: an inflow stream of lake Wular (Ramsar Site), Kashmir Himalaya. J. Ecosyst. 2014; 2014:1-18.
38. Yang K., Yu Z., Luo Y., Yang Y., Zhao L., Zhou X. Spatial and temporal variations in the relationship between lake water surface temperatures and water quality - A case study of Dianchi Lake. Sci. Total. Environ. 2018; 624:859-871.
39. Patil V.B.B., Pinto S.M., Govindaraju T., Hebbalu V.S., Bhat V., Kannanur L.N. Multivariate statistics and water quality index (WQI) approach for geochemical assessment of groundwater quality—a case study of Kanavi Halla Sub-Basin, Belagavi, India. Environ. Geochem. Hlth. 2020; 42(9):2667-2684.
40. Bean T.A., Sumner P.D., Boojhawon R., Tatayah V., Khadun A.K., Hedding D.W., Rughooputh SDDV, Nel W. Bedrock-incised gully erosion phenomena on Round Island, Mauritius. Catena 2017;151:107-117.
41. Zeinalzadeh K., Rezaei E. Determining spatial and temporal changes of surface water quality using principal component analysis. J. Hydrol. Reg. Stud. 2017; 13:1-10.
42. Simeonov V., Stratis J., Samara C., Zachariadis G., Voutsa D., Anthemidis A., Sofoniou M., Kouimtzis T.H. Assessment of the surface water quality in Northern Greece. Water. Res.2003;37(17):4119-4124.
43. Zheng L.-y., Yu H.-b., Wang Q.-s. Assessment of temporal and spatial variations in surface water quality using multivariate statistical techniques: A case study of Nenjiang River basin, China. J. Cent. South. Univ. 2015; 22(10):3770-3780.
44. Mukherjee I., Singh U.K.J.E.g., health. Groundwater fluoride contamination, probable release, and containment mechanisms: a review on Indian context. Environ. Geochem. Health 2018; 40(6):2259-2301.
45. Zhang Q., Li L., Sun R., Zhu D., Zhang C., Chen Q. Retrieval of the soil salinity from Sentinel-1 Dual-Polarized S.A.R. data based on deep neural network regression. IEEE Geosci. Remote S. 2020; 19:1-5.
46. Kurunc A., YÜREKLİ K., ÖZTÜRK F. Effect of discharge fluctuation on water quality variables from the Yeşilırmak River. J. Agric. Sci. 2005; 11(02):189-195.
47. Ejaz N. Investigation of the Soan River Water

[DOI: 10.22034/ECOPERSIA.12.3.283]

Quality Using Multivariate Statistical Approach. Int. J. Photoenergy 2020; 2020.
48. Ouyang Y., Nkedi-Kizza P., Wu Q., Shinde D., Huang C. Assessment of seasonal variations in surface water quality. Water Res. 2006; 40(20):3800-3810.
49. Olsen R.L., Chappell R.W., Loftis J.C. Water quality sample collection, data treatment, and results presentation for principal components analysis–literature review and Illinois River watershed case study. Water Res. 2012; 46(9):3110-3122.
50. Piper A.M. A graphic procedure in the geochemical interpretation of water-analyses. Eos, Trans. Am. Geophys. Union. 1944; 25(6):914-928.
51. Clow D.W., Striegl R.G., Dornblaser M. Spatiotemporal dynamics of CO2 gas exchange from headwater mountain streams. J. Geophys. Res.-Biogeo. 2021; 126(9):e2021JG006509.
52. Razi M.H., Wilopo W., Putra DPE Hydrogeochemical evolution and water-rock interaction processes in the multilayer volcanic aquifer of Yogyakarta-Sleman Groundwater Basin, Indonesia. Environ. Earth Sci. 2024; 83(6):164.
53. Boulom J., Putra D.P.E., Wilopo W. Chemical composition and hydraulic connectivity of springs in the Southern Slope of Merapi Volcano. J. Appl. Geol. 2015; 6(1).
54. Cloutier V., Lefebvre R., Therrien R., Savard M.M. Multivariate statistical analysis of geochemical data as indicative of the hydrogeochemical evolution of groundwater in a sedimentary rock aquifer system. J. Hydrol. 2008; 353(3-4):294-313.
55. Rezaei Moghaddam M.H., Nikjoo M.R., Hejazi M.A., Khazri S., Kazemi A. The Effect of Hydrogeomorphological Factors on SiminehRood River Water Quality Changes at Different Study Stations during the Years 2003-2002. J. Hydrol. 2017; 4(2):395-405.
56. Kardan Moghaddam H., Javadi S., Roozbehani R., Mohammadi Ghale Ney M. Rivers riparian buffer zones determination by combining USDA and qualitative vulnerability (Case study: Ab-Shirin river). JSCR. 2018; 25(4):113-132.
57. Heshmati M., Gheitury M., Garibreza M. Quality of river water for irrigation and drinking uses and sources of contamination in upper catchment areas. ECOPERSIA 2021; 10;9(2):119-129.
58. Kaveh A.R., Habibnejad Roshan M., Shahedi K., Ghorbani J. Evaluation of temporal and spatial changes in water quality (Case Study: River Talar, Mazandaran Province). 2013; Sixth year: 49- 62. J. Water Resour. Eng. 2013; 6(18):49-62. (In Persian)
59. Davoudi Moghaddam D., Haghizadeh A., Tahmasebipour N., Zeinivand H. Spatial and temporal water quality analysis of a semi-arid river for drinking and irrigation purposes using water quality indices and GIS ECOPERSIA 2021; 9(2):79-93.

[DOI: 10.22034/ECOPERSIA.12.3.283]